

# OFDM-based wideband hybrid beamformer for mmWave massive MIMO multiuser 5G systems

Faez Fawwaz Shareef<sup>1,2</sup>, Manal Jamil Al-Kindi<sup>2</sup>

<sup>1</sup>Department of Communication Engineering, University of Technology Iraq, Baghdad, Iraq

<sup>2</sup>Department of Electronic and Communication Engineering, College of Engineering, Al-Nahrain University, Baghdad, Iraq

## Article Info

### Article history:

Received Sep 18, 2022

Revised Nov 2, 2022

Accepted Nov 20, 2022

### Keywords:

Block diagonalization

Hybrid beamformer

Massive MIMO

Matching pursuit

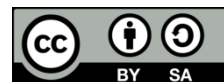
Spatially sparse precoder

Wideband channel

## ABSTRACT

Employing massive antennas array at the user terminals can be feasible by using millimeter wave (mmWave) transmission which significantly reduce the antennas array size. The implementation of massive multiple input multiple output (MIMO) at the user terminals facilitates accurate beamforming. In this paper, a modified orthogonal matching pursuit (OMP) algorithm is used to design a wideband hybrid combiner based on the sparse structure of mmWave channel and orthogonal frequency-division multiplexing (OFDM). Based on OFDM, the wideband channel considered as multiple narrowband channels so a modified narrowband hybrid combiner can be implemented for each subcarrier channel in a manner where the RF combiner is the same for all subcarriers, whilst the baseband combiner is obtained for each subcarrier. For the multiuser 5G system, a wideband hybrid precoder based on the block diagonalization (BD) method is used at the base station (BS) to cancel the interference at each user due to the other users. The performance of this hybrid beamformers (precoder/combiner) are tested for different scenarios of base station antennas number, numbers of users' antennas, and number of users.

This is an open access article under the [CC BY-SA](#) license.



## Corresponding Author:

Faez Fawwaz Shareef

Department of Communication Engineering, University of Technology  
Baghdad, Iraq

Email: faez.f.shareef@uotechnology.edu.iq

## 1. INTRODUCTION

The main technology of the fifth generation (5G) system is the large-scale antenna array. Massive multiple input multiple output (MIMO) system is a large-scale antennas array with huge antennas numbers up to several hundreds or thousands [1], [2]. Massive MIMO system increases the system capacity and provide more reliability to communication link leading to enhance energy and spectral efficiencies of the system. In massive MIMO, a huge number of antennas can be implemented at base station (BS) [3]–[5]. However, it is difficult to apply large number of antennas at the user terminals due to the large physical size of antenna. For example, the size of (4×4) uniform planar array (UPA) operates at a 5 GHz frequency is about 80 cm<sup>2</sup>. Whilst using millimeter-wave transmission (mmWave) leads to more realistic implementation of the massive MIMO technology at the user terminals [6], [7]. It can be seen that the size of the UPA mentioned above can be reduced to about 2.6 cm<sup>2</sup> when the operating frequency is 28 GHz, even so about (16×16) UPA can be implemented in the 80 cm<sup>2</sup> area when operates at 28 GHz which provide more accurate beamforming [8], [9].

Analog beamformer is a beamformer implemented at the radio frequency (RF) stage, while digital beamformer implemented at the baseband stage [10]. The analog beamformer uses phase shifters to aim the main beam toward the desired direction [10], [11]. The beamforming process in the digital beamformer is

accomplished by means of the digital signal processing. It is kindly easy to do the beamforming process using digital beamformer with more accuracy and flexibility rather than analog beamformer [12]. However, a dedicated RF chain is required for each antenna element in digital beamforming. This RF chain module contains analog-to-digital converter (ADC), digital-to-analog converter (DAC), power amplifier, and mixers which makes its design at mmWave complex and expensive and large number of antennas are used [13], [14].

A structure of both digital and analog beamformers was introduced to take advantage of the both types of beamforming, and this combination called hybrid beamforming [15], [16]. Hybrid beamforming was mentioned for the first time in [17]. In hybrid beamforming, the antennas of array divided into many subarrays each connected to one RF chain only. So, the number of RF chains is significantly reduced, leading to a cheap and a simple system design. The performance gap between fully digital and hybrid beamformers can be reduced by optimizely design the hybrid beamformer. Also if the number of chains is more than two times the number of data, the gap becomes negligible [10], [18].

The amplitude and phase of the transmitted symbols can be modified using the digital beamformer, but the analog beamformer can modify only the phase of the transmitted symbols because it has a constant amplitude  $1/\sqrt{N_t}$ . In fact, the analog beamformer has quantized phases of N bits resolution, so accurate analog beamforming required a high resolution phase shifter which needed more bits [19], [20]. In this paper, a new design of wideband hybrid beamformer based on orthogonal frequency-division multiplexing (OFDM) is proposed for a massive MIMO multiuser 5G system. Since the mmWave channel is specular and has a sparse structure, the beamforming design problem can be formulate as a sparse reconstruction problem [21]. a modified algorithm of orthogonal matching pursuit (OMP) algorithm is used to find the optimal wideband hybrid combiner. The wideband 5G channel is divided into multiple narrowband channels by means of OFDM technique, so the proposed combiner can be applied to each subchannel. To eliminate the interferences between users, block diagonalization (BD) is used at the BS as a wideband hybrid precoder according to the modified joint spatial division multiplexing (JSDM) design mentioned in [12]. The design separation between precoder and combiner is accomplished giving Kronecker channel model [22], [23].

The following notation are used here:  $(\cdot)^{-1}$ ,  $(\cdot)^*$  and  $(\cdot)^H$  denote the inverse, conjugate and conjugate transpose respectively;  $\|\cdot\|_\ell$  and  $\|\cdot\|_F$  are  $\ell$ -norm and Frobenius norm respectively. Statistical expectation is denoted by  $\mathbb{E}[\cdot]$ ;  $\text{diag}(\cdot)$  is the diagonal elements;  $\mathcal{CN}(m, \mathcal{M})$  is a complex Gaussian distribution with mean  $m$  and covariance matrix  $\mathcal{M}$ ;  $\text{span}(\mathcal{V})$  and  $\text{span}^\perp(\mathcal{V})$  are the column space of  $(\mathcal{V})$  and its orthogonal complement respectively. SVD is the singular value decomposition and EVD is the eigen value decomposition.

## 2. SYSTEM MODEL

Consider a downlink multiuser MIMO-OFDM 5G system, shown in Figure 1, operates at mmWave frequency 28 GHz, where BS supplied with  $N_t$  antennas placed in an UPA. The BS communicates with  $N_u$  users through  $N_s$  independent data streams such that  $N_s = \sum_{i=1}^{N_u} N_{s,i}$ , and  $N_{s,i}$  represents the streams per user. Each user equipped with  $N_{r,i}$  antennas so  $N_r = \sum_{i=1}^{N_u} N_{r,i}$ .  $N_{RF}^t$ ,  $N_{RF,i}^t$ ,  $N_{RF}^r$ , and  $N_{RF,i}^r$  are the total number of RF chain at the BS, the number of dedicated RF chain at the BS for the  $i^{th}$  user, the total number of the receiver RF chain of all users, and the number of receiver RF chain for  $i^{th}$  user respectively. Working at the mmWave band can enhance the beamforming and transmission bit rate, but to obtain these benefits, OFDM is needed to deal with the large wideband of mmWave channel by dividing this wideband channel into several narrowband channels, so a conventional narrowband beamformer can be applied to this system [12], [24].

The hybrid precoder is applied at the BS, while the hybrid combiner is applied at the user terminals. At both side of the transmission link, the analog precoder/combiner is common over all subcarrier channels, and the digital beamformer is applied to each subchannel.  $f_i^k$  and  $\omega_i^k$  are the hybrid subcarrier precoder and hybrid subcarrier combiner of the  $k^{th}$  subcarrier channel for  $i^{th}$  user respectively. The  $f_i^k$  of the  $k^{th}$  subchannel is of the form  $F_{RF,i} f_{BB,i}^k$ , where analog precoder  $F_{RF,i} \in \mathbb{C}^{N_t \times N_{RF,i}^t}$ , and baseband precoder  $f_{BB,i}^k \in \mathbb{C}^{N_{RF,i}^t \times N_{s,i}}$ . The  $\omega_i^k$  is of the form  $W_{RF,i} \omega_{BB,i}^k$ , where  $W_{RF,i} \in \mathbb{C}^{N_{r,i} \times N_{RF,i}^r}$  is the analog combiner, and  $\omega_{BB,i}^k \in \mathbb{C}^{N_{RF,i}^r \times N_{s,i}}$  is the digital combiner.

In this paper, the focus is on the design of the hybrid subcarrier combiner while adopting the design mentioned in [12] for the hybrid subcarrier precoder. In fact, the design of the hybrid subcarrier precoder/combiner can be separable as will be showed later. The digital subcarrier precoder  $f_{BB,i}^k$  maps the transmitted symbol signal  $x_i^k$  of  $k^{th}$  subcarrier and belongs to  $i^{th}$  user to the input of OFDM transmitter, then  $N_{RF,i}^t$  RF chains is used to upconvert the OFDM signal to RF stage. Finally, the output of the chains is

connected to the BS antennas array using  $N_{RF,i}^t \times N_t$  phase shifters of the analog precoder  $F_{RF,i}$  because of using the fully connected structure.

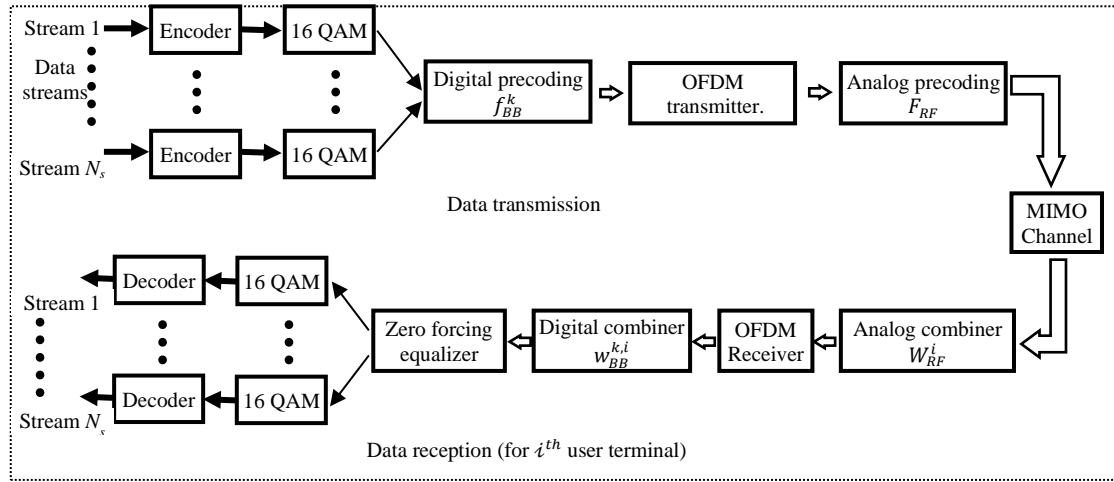


Figure 1. Multi-stream multi-user massive MIMO-OFDM 5G system

So, the transmitted signal  $y_i^k$  as (1):

$$y_i^k = F_{RF,i} f_{BB,i}^k x_i^k \quad (1)$$

The received signal, before the hybrid subcarrier combiner,  $r_i^k$  at  $i^{th}$  user as (2):

$$r_i^k = \sqrt{\mathcal{P}_i} H_i^k F_{RF,i} f_{BB,i}^k x_i^k + \sum_{\substack{j=1 \\ j \neq i}}^{N_u} \sqrt{\mathcal{P}_j} H_i^k F_{RF,j} f_{BB,j}^k x_j^k + n_i \quad (2)$$

The noise signal  $n_i$  has complex gaussian distribution e.g.,  $n_i \sim \mathcal{CN}(0, \mathcal{R}n_i)$ ,  $\mathcal{R}n_i$  is the covariance matrix, and the average power at the  $i^{th}$  user is  $\mathcal{P}_i$ . The wideband channel  $H_i^k \in \mathbb{C}^{N_{r,i} \times N_t}$  between BS and the  $i^{th}$  user at  $k^{th}$  OFDM subcarrier [25]. Following the approach of [12], the MIMO channel  $H_i^k$  becomes as (3):

$$H_i^k \approx \gamma_i \sum_{\ell}^{N_{cl,i}} \sum_m^{N_{\ell,i}} \beta_{\ell,m,k,i} a_{r,i}(\phi_{\ell,m,i}^r, \theta_{\ell,m,i}^r) a_t^H(\phi_{\ell,m,i}^t, \theta_{\ell,m,i}^t) \quad (3)$$

This channel model consists of  $N_{cl,i}$  clusters, and  $N_{\ell,i}$  rays per  $\ell^{th}$  cluster, so  $N_{rays,i} = \sum_{\ell=1}^{N_{cl,i}} N_{\ell,i}$ .  $\gamma_i = \sqrt{N_t N_r / N_{rays,i}}$ , and  $\beta_{\ell,m,k,i}$  is the complex gain of the  $m^{th}$  ray in the  $\ell^{th}$  cluster at the  $k^{th}$  subchannel, whereas  $\phi_{\ell,m,i}^r(\theta_{\ell,m,i}^r)$  is the azimuth (elevation) angle of arrival whilst  $\phi_{\ell,m,i}^t(\theta_{\ell,m,i}^t)$  is the azimuth (elevation) angle of departure.  $a_t(\cdot)$  and  $a_{r,i}(\cdot)$  are the antennas array response vectors of BS and the  $i^{th}$  user respectively. The right hand of (3) is similar to the narrowband channel model [26], so a narrowband beamformer can be applied for each OFDM subcarrier. For simplicity, the following assumption are made: each user has the same number of data streams, so  $\{\mathcal{P}_i = \mathcal{P}, \forall i\}$ ,  $x_i^k$  has a normal distribution e.g.,  $x_i \sim \mathcal{N}(0, \mathcal{R}x_i)$ , the covariance matrix  $\mathcal{R}x_i = 1/N_{S,i} I_{N_{S,i}} \cdot \{ \|F_{RF,i} f_{BB,i}^k\|_F^2 = N_{S,i}, \forall k, i \}$  for the transmitted power constraint. Assume  $r_i^k$  propagates through a block fading narrowband channel, this assumption is true as long as using OFDM technique [24], [27]. Moreover, based on the Kronecker channel model [22], [28] the hybrid subcarrier precoder and combiner can design separately.

### 3. HYBRID BEAMFORMING DESIGN

The essential key in the design of hybrid beamforming is finding the optimal precoder and combiner weights  $f_{BB,i}^k, F_{RF,i}, w_{BB,i}^k, W_{RF,i}$  that minimize the mean square error (MSE) between transmitted and

received symbols for all users and over all subcarriers. As mentioned earlier it is acceptable to firstly design the hybrid subcarrier precoder then the hybrid subcarrier combiner. The design of hybrid precoder and combiner is described in the following sub-sections.

### 3.1. Hybrid subcarrier precoder design

The JSDM algorithm [29] and its modification [12] show a little performance degradation in comparison to the optimal fully digital precoder and reduce the overhead information needed to feed back, so this algorithm is adopted here to design the hybrid subcarrier precoder for the system in Figure 1. The users assumed to be distributed in a manner that they are well-spatially separated and there is only one user per group. The powerful of this algorithm is that the analog precoder design depends on the second-order statistics of the channel and not on its first order statistics. The analog precoder  $F_{RF,i}$  is designed according to the procedures listed in Algorithm 1 [12].

Algorithm 1: design of analog precoder  $F_{RF,i}$

1. Estimate  $H_i^k$ .
2. Define  $\mathcal{M}_i^k = \mathbb{E}[H_i^k H_i^{kH}]$ .
3. Find the eigenvectors  $\mathcal{V}_i^k$  by computing EVD( $\mathcal{M}_i^k$ ).
4. Feedback  $\mathcal{V}_i^k$  to the BS.
5. Computing  $\bar{\mathcal{V}}_i$  by averaging  $\mathcal{V}_i^k$  over all subchannels.
6. Define  $\Xi_i = [\bar{\mathcal{V}}_i \bar{\mathcal{V}}_i \dots \bar{\mathcal{V}}_{i-1} \bar{\mathcal{V}}_{i+1} \dots \bar{\mathcal{V}}_{N_u-1} \bar{\mathcal{V}}_{N_u}]^T$ .
7. Find the eigenvectors  $\mathfrak{B}_i$  by computing SVD( $\Xi_i$ ).
8. Define  $\mathfrak{B}_i^{(0)}$  such that  $\text{Span}(\mathfrak{B}_i^{(0)}) = \text{Span}^\perp(\{\Xi_j: \forall j \neq i\})$ .
9. BS broadcasts  $\mathfrak{B}_i^{(0)}$  for all users.
10. Define  $\mathcal{H}_i^k = H_i^k \mathfrak{B}_i^{(0)}$ .
11. Define  $\hat{\mathcal{M}}_i^k = \mathbb{E}[\mathcal{H}_i^k \mathcal{H}_i^{kH}]$ .
12. Find the eigenvectors  $\hat{\mathcal{V}}_i^k$  by computing EVD( $\hat{\mathcal{M}}_i^k$ ).
13. Computing  $\bar{\mathcal{V}}_i$  by averaging  $\hat{\mathcal{V}}_i^k$  over all subchannels.
14. Find  $\bar{\mathcal{V}}_i^{(1)}$  such that  $\bar{\mathcal{V}}_i = [\bar{\mathcal{V}}_i^{(1)} \bar{\mathcal{V}}_i^{(0)}]$ .
15. Finally, the analog precoder is defined,  $F_{RF,i} = \mathfrak{B}_i^{(0)} * \bar{\mathcal{V}}_i^{(1)}$ .

Now, the channel is defined as  $\tilde{H}_i^k = H_i^k F_{RF,i}$ , and its covariance matrix is  $\tilde{\mathcal{M}}_i^k = F_{RF,i}^H \mathcal{M}_i^k F_{RF,i}$ . Since,  $F_{RF,i}^H F_{RF,i} \approx c I_{N_{RF,i}^t}$  for large number of BS antennas [21], [24], the digital subcarrier precoder  $f_{BB,i}^k$  is the normalized  $N_{s,i}$  eigenvectors of  $\tilde{\mathcal{M}}_i^k$ .

### 3.2. Hybrid subcarrier combiner design

Since the hybrid subcarrier combiner design is independent for each user but it is the same for all users. Therefore, the procedures of the design discussed here are for  $i^{th}$  user only. The second term of the right-hand side of (2) is eliminated because the column vectors of  $F_{RF,i}$  eliminates inter-group interference between users [30], and (2) as (4):

$$r_i^k = \sqrt{\mathcal{P}_i} H_i^k F_{RF,i} f_{BB,i}^k x_i^k + n_i \quad (4)$$

By applying the hybrid subcarrier combiner  $\omega_i^k$ , the received signal  $r_i^k$  in (5):

$$\begin{aligned} r_i^k &= \omega_i^{kH} r_i^k \\ &= \sqrt{\mathcal{P}_i} \omega_{BB,i}^k H_i^k F_{RF,i} f_{BB,i}^k x_i^k + \omega_{BB,i}^k H_i^k F_{RF,i} n_i \end{aligned} \quad (5)$$

The hybrid subcarrier combiner is designed to minimize the MSE between  $x_i^k$ , and  $r_i^k$ . The optimization problem is written as (6):

$$\begin{aligned} (W_{RF,i}^{opt}, \omega_{BB,i}^{k,opt}) &= \arg \min_{W_{RF,i}, \omega_{BB,i}^k} \mathbb{E} [\|x_i^k - r_i^k\|_2^2] \\ s.t. W_{RF,i} &\in \mathbb{W}_{RF} \end{aligned} \quad (6)$$

Where  $W_{RF,i}^{opt}, \omega_{BB,i}^{k,opt}$  are the optimal values of the analog combiner and digital subcarrier combiner respectively.  $\mathbb{W}_{RF}$  is the feasible set of analog combiners. The optimal unconstrained solution  $\omega_i^{k,opt}$  of (6) is well known [31] as (7):

$$\begin{aligned}
\omega_i^{k,opt} &= \left[ \mathbb{E} \left[ x_i^k r_i^{kH} \right] \mathbb{E} \left[ r_i^k r_i^{kH} \right]^{-1} \right]^H \\
&= \left[ \frac{\sqrt{\mathcal{P}_i}}{N_{s,i}} f_{BB,i}^k F_{RF,i}^H H_i^k \left( \frac{\mathcal{P}_i}{N_{s,i}} H_i^k F_{RF,i} f_{BB,i}^k f_{BB,i}^k F_{RF,i}^H H_i^k + \sigma_{n,i}^2 I_{N_{r,i}} \right)^{-1} \right]^H \\
&\stackrel{(a)}{=} \left[ \frac{1}{\sqrt{\mathcal{P}_i}} \left( f_{BB,i}^k F_{RF,i}^H H_i^k F_{RF,i} f_{BB,i}^k + \frac{\sigma_{n,i}^2 N_{s,i}}{\mathcal{P}_i} I_{N_{s,i}} \right)^{-1} f_{BB,i}^k F_{RF,i}^H H_i^k \right]^H
\end{aligned} \tag{7}$$

Where (a) is obtained by applying the push-through identity of matrix inversion lemmas. In order to apply this optimal combiner  $\omega_i^{k,opt}$  to the system of Figure 1, this combiner needs to be decomposed into the product of analog and digital subcarrier combiner  $W_{RF,i}^{opt} \omega_{BB,i}^{k,opt}$  with  $W_{RF,i} \in \mathbb{W}_{RF}$ . Due to this complex non-convex constraint, there is no optimal solution of (6). Since each subcarrier channel is modelled as a narrowband channel, the approach of [21] is applied here to overcome this difficulty. According to this approach the optimization problem can be rewritten as (8).

$$\begin{aligned}
(W_{RF,i}^{opt}, \omega_{BB,i}^{k,opt}) &= \arg \min_{W_{RF,i}, \omega_{BB,i}^k} \left\| \mathbb{E} \left[ r_i^k r_i^{kH} \right]^{\frac{1}{2}} (\omega_i^{k,opt} - W_{RF,i} \omega_{BB,i}^k) \right\|_F \\
s.t. \quad W_{RF,i} &\in \mathbb{W}_{RF}
\end{aligned} \tag{8}$$

Now the optimization problem is to find the  $\mathbb{E} \left[ r_i^k r_i^{kH} \right]$ -weighted Frobenius norm projection of the unconstrained combiner  $\omega_i^{k,opt}$  onto the set of hybrid subcarrier combiners of the form  $W_{RF,i} \omega_{BB,i}^k$  with  $W_{RF,i} \in \mathbb{W}_{RF}$ . Again, the feasibility constrain makes the solving of (8) very difficult. Fortunately, due to the sparse structure of  $H_i^k$ , a near optimal combiner can be found by more restricting  $W_{RF,i}$  so its columns are  $N_{RF,i}^r$  columns of an  $N_{r,i} * N_{rays,i}$  matrix of receiver array response vectors  $A_{r,i} = [a_{r,i}(\phi_{1,1,i}^r, \theta_{1,1,i}^r), a_{r,i}(\phi_{N_{c\ell,i}, N_{\ell,i,i}}^r, \theta_{N_{c\ell,i}, N_{\ell,i,i}}^r)]$  and solving as (9).

$$\begin{aligned}
\tilde{\omega}_{BB,i}^{k,opt} &= \arg \min_{\tilde{\omega}_{BB,i}^k} \left\| \mathbb{E} \left[ r_i^k r_i^{kH} \right]^{\frac{1}{2}} (\omega_i^{k,opt} - A_{r,i} \tilde{\omega}_{BB,i}^k) \right\|_F \\
s.t. \quad \left\| \text{diag} \left( \tilde{\omega}_{BB,i}^k \tilde{\omega}_{BB,i}^{kH} \right) \right\|_0 &= N_{RF,i}^r
\end{aligned} \tag{9}$$

Algorithm 2: design of hybrid subcarrier combiner  $\omega_i^k$

- A. for  $k \leq \text{number of OFDM subcarrier}$  do
  - a. Initialization
    1. Estimate  $H_i^k$
    2. Find  $f_{BB,i}^k$  and  $F_{RF,i}$  according to Algorithm 1
    3. Compute  $\omega_i^{k,opt}$  according to (7)
    4. Let  $\mathcal{W}_{RF,i}^k$  be an empty matrix
    5. Compute  $\mathcal{E}_i^k = \mathbb{E} \left[ r_i^k r_i^{kH} \right]$
    6. Set  $\omega_{res}^{(0)} = \omega_i^{k,opt}$
  - b. Construction of  $\omega_{BB,i}^k$  and  $\mathcal{W}_{RF,i}^k$ 
    1. for  $J = 1, 2, N_{RF,i}^r$  do
      2.  $\Phi = A_{r,i} \mathcal{E}_i^k \omega_{res}^{(J-1)}$
      3.  $\mathcal{L} = \arg \max(\text{diag}(\Phi \Phi^H))$
      4. Add  $\mathcal{L}^{th}$  column of  $A_{r,i}$  to  $\mathcal{W}_{RF,i}^k$
    5. Using least squares (LS) to find  $\omega_{BB,i}^k = (\mathcal{W}_{RF,i}^k \mathcal{E}_i^k \mathcal{W}_{RF,i}^k)^{-1} \mathcal{W}_{RF,i}^k \mathcal{E}_i^k \omega_i^{k,opt}$
    6.  $\omega_{res}^{(J)} = \frac{\omega_i^{k,opt} - \mathcal{W}_{RF,i}^k \omega_{BB,i}^k}{\left\| \omega_i^{k,opt} - \mathcal{W}_{RF,i}^k \omega_{BB,i}^k \right\|_F}$
    7. end for
      2. end for
  - c. Construction of  $W_{RF,i}$  by taking the mean of  $\mathcal{W}_{RF,i}^k$  over all subcarriers

Now the problem is equivalent to sparse signal recovery problem and can be solved through OMP [21].  $\tilde{\omega}_{BB,i}^k \in \mathbb{C}^{N_{rays,i} * N_s}$  acts as an auxiliary variable from which the digital subcarrier combiner is obtained. The constrain  $\left\| \text{diag} \left( \tilde{\omega}_{BB,i}^k \tilde{\omega}_{BB,i}^{kH} \right) \right\|_0 = N_{RF,i}^r$  ensure that the  $\tilde{\omega}_{BB,i}^k$  cannot have more than  $N_{RF,i}^r$  non-zero

rows which form the digital subcarrier combiner  $\omega_{BB,i}^k$ , thus only  $N_{RF,i}^r$  columns of  $A_{r,i}$  is effectively selected to construct the analog combiner  $W_{RF,i}$ . The complete design of hybrid subcarrier combiner  $\omega_i^k$  is illustrated in Algorithm 2.

#### 4. RESULTS AND DISCUSSION

In this section, the performance of Algorithms 1 and 2 of the hybrid subcarrier beamformers  $f_i^k$  and  $\omega_i^k$  design is evaluated considering the system in Figure 1. Different numbers of users randomly distributed within a one-thousand-meter diameter are used to test the performance of these algorithms. To ease the calculations, all users are equipped with the same number of antennas and communicates two data streams  $N_{s,i} = 2$  with BS. The wideband 28 GHz channel is dividing into 256 OFDM subchannels plus 64 cyclic-prefix (CP). The clustered channel in (3) is adopted to model these subchannels, so each subchannel consist of ten clusters each with ten rays. For channel estimation a channel sounding system is used. The results of proposed algorithm are compared to that of fully digital beamformer for different numbers of BS array antennas, also different numbers of users' array antennas are used to test the system in Figure 1. The antennas of both BS and users' array are arranged in UPA, and the number of transmitted RF chain is 3 per data stream,  $N_{RF,i}^t = 3 \times N_{s,i}$ , and the receiver RF chain is one per data stream,  $N_{RF,i}^r = N_{s,i}$ .

First, a comparison between a fully digital beamformer with full channel state information (FCSI,FD) and the proposed beamformer which designed based on Algorithms 1 and 2 is presented in Figure 2 in term of average spectral efficiency versus signal-to-noise ratio (SNR). The comparison is done for a various number of BS antennas  $N_t=64, 128$  and  $256$ , and the number of users is six. In Figure 2(a) The number of antennas per user is four, whilst is six for Figure 2(b). The performance of the proposed beamformer (Algorithms 1 and 2) is also compared with that of the precoder designed using Algorithm 1 to show the enhancement obtained by applying the combiner at the users' terminals.

As shown in Figure 2, increasing the number of BS antennas reduces the gap between FCSI,FD and Algorithms 1 and 2. Also, it has been shown that the performance of Algorithms 1 and 2 superiors to that of Algorithm 1 especially when the number of users' antennas increases which means that the applying of combiner at users will enhance the system in Figure 1. So, the gap between Algorithm 1, Algorithms 1 and 2 is about 0.97 at SNR=10 dB for  $N_t = 64$  antennas and  $N_{r,i} = 4$  antenna, but the gap increases to be approximately 1.5 when the number of users' antennas is increased to be 8 antennas. Moreover, the performance gap between Algorithms 1, 2 and Algorithm 1 is more when the number of BS antennas is low, e.g.,  $N_t = 64$ , so it is found that the gap is about 1.5 at SNR=10 dB for  $N_t = 64$  and  $N_{r,i} = 8$  whilst the gap is about 1.2 when  $N_t = 256$ . It means that the proposed Algorithms 1 and 2 provides more spectral efficiency for system with low number of BS antennas.

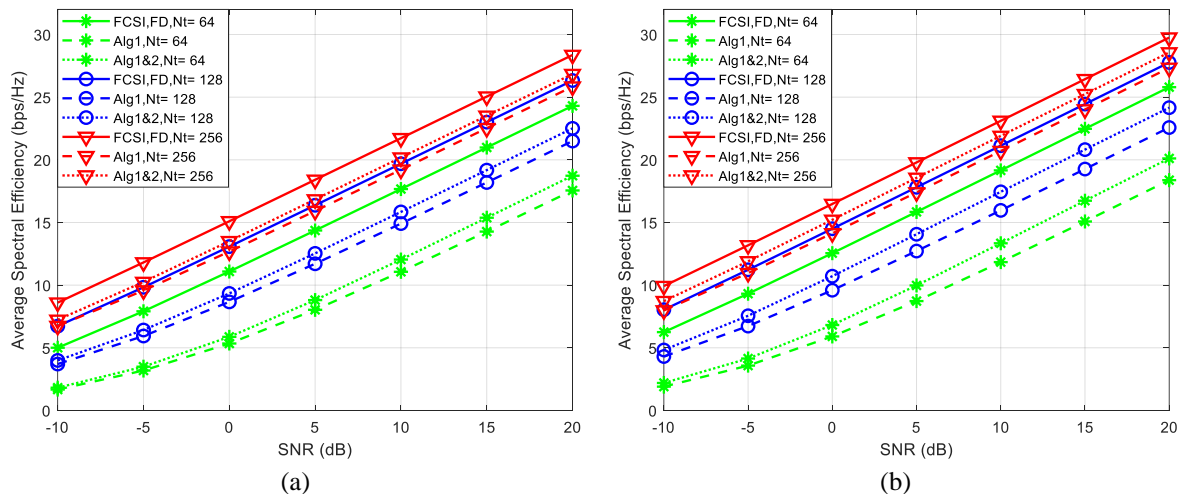


Figure 2. Spectral efficiency of FCSI,FD, Algorithm 1, Algorithms 1 and 2 for six users, each user equipped with; (a) four antennas, and (b) eight antennas, two data stream per user

Figure 3 shows the performance of FCSI,FD, Algorithm 1, Algorithms 1 and 2 for the system when  $N_u = 6$  users, and  $N_{r,i} = 16$  antennas for 128, and 256 BS antennas. The system with 64 BS antennas can't

be implemented here because the total number of users' antennas,  $N_r = 96$ , is more than that of BS. Here, the performance gap is about 1.89 when  $N_t = 128$ , while it is about 1.2 when  $N_t = 256$ . Again, it has been shown that increasing the number of users' antennas enhances the performance of Algorithms 1 and 2 and reduce the gap with FCSI-FD. To study the effect of the number of users' antennas on the system in Figure 1, the spectral efficiency versus number of antennas per user,  $N_{r,i} = 4, 8, 16$ , and 32, is plotted in Figure 4 for different number of users and BS antennas where the SNR=5 dB.

The results of Figure 4 prove that the performance of Algorithms 1 and 2 is superior to that of Algorithm 1 specifically when increasing the number of antennas per user. The enhancement of Algorithms 1 and 2 is about 1.16 above Algorithm 1 when  $N_t = 256$ ,  $N_u = 6$ , and  $N_{r,i} = 8$ . Correspondingly the enhancement increases to about 1.4 when  $N_{r,i} = 16$ , and exceeds 2 for  $N_{r,i} = 32$ . Again, the system with  $N_t = 128$  cannot implemented when the number of antennas per user  $N_{r,i} = 32$ , because the total number of users' antennas  $N_r = 192$  which is much more than the number of BS antennas.

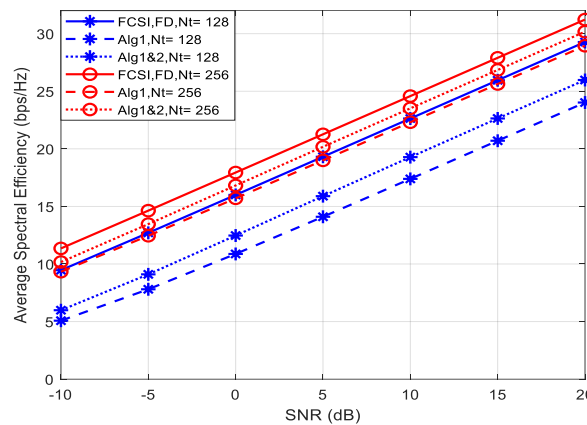


Figure 3. Spectral efficiency of FCSI-FD, Algorithm 1, Algorithms 1 and 2 for six users; each user equipped with sixteen antennas, two data stream per user

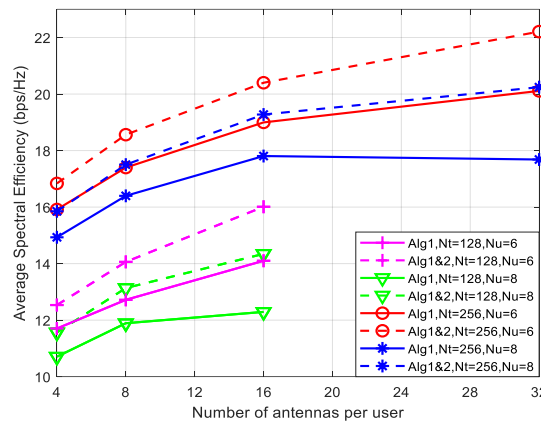


Figure 4. Spectral efficiency of Algorithm 1, Algorithms 1 and 2 versus number of antennas per user for six and eight users

Moreover, it shown that the performance of Algorithms 1 and 2 when  $N_u = 8$  is approximately the same as that of Algorithm 1 when  $N_u = 6$  for either 128 or 256 BS antennas despite that the performance reduces as the number of user increases. The relation between spectral efficiency and the number of users is illustrated in Figure 5. Here, it can be shown that the performance of the system in Figure 1 decreases as the number of users increases. However, the performance of Algorithms 1 and 2 when  $N_{r,i} = 8$  is almost the same as the performance of Algorithm 1 when  $N_{r,i} = 16$  for both 128 and 256 BS antennas. This means that applying the proposed combiner designed based on Algorithm 2 either enhances the system or decreases the number of users' antennas required to achieve a certain sum rate.

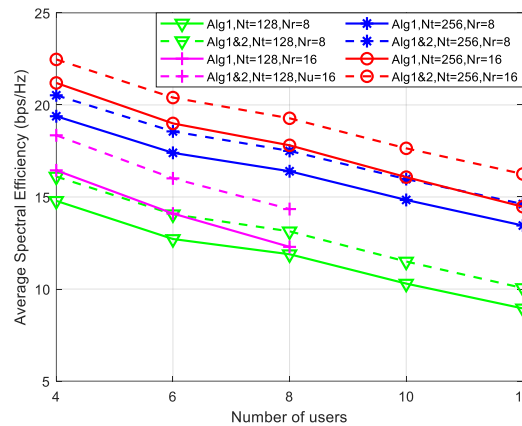


Figure 5. Spectral efficiency of Algorithm 1, Algorithm 1 and 2 versus number of users

## 5. CONCLUSION

In this paper, an OFDM-based wideband hybrid subcarrier beamformer is designed for multi users MIMO 5G system. The design consists of two stages. In the first stage, the hybrid subcarrier precoder is designed based on the concepts of BD, whereas the hybrid subcarrier combiner is designed based on the concept of sparse signal recovery. Both the precoder and combiner is designed for wideband mmWave system through using OFDM technique to deal with this wideband channel as multiple narrowband channels. This wideband beamformer has been tested for a massive MIMO 5G system where the effects of the number of BS antennas, the number of antennas per user and the number of users on the performance of the proposed beamformer are evaluated. The results show that the proposed beamformer has an acceptable degradation in spectral efficiency in comparison to the performance of the fully digital beamformer with full CSI. Also, they show that the proposed beamformer (combiner plus precoder) provides good enhancement in comparison to a system applying precoder only where the enhancement of the spectral efficiency exceeds two when the number of antennas per user is more than 32. Despite the proposed beamformer is not an optimal beamformer but it provides a good performance in term of spectral efficiency and computational efficiency because it depends on the second channel statistics which are change slowly with time, so this eventually reduces the overhead information need to deal with them.

## REFERENCES

- [1] C. -R. Tsai, Y. -H. Liu, and A. -Y. Wu, "Efficient compressive channel estimation for millimeter-wave large-scale antenna systems," *IEEE Transactions on Signal Processing*, vol. 66, no. 9, pp. 2414–2428, May 2018, doi: 10.1109/TSP.2018.2811742.
- [2] Y. E. Gholb and N. E. A. E. Idressi, "5G mobile antennas: MIMO implementation," in *2019 International Conference on Wireless Technologies, Embedded and Intelligent Systems (WITS)*, Apr. 2019, pp. 1–6, doi: 10.1109/WITS.2019.8723661.
- [3] R. Dong, A. Li, W. Hardjawana, Y. Li, X. Ge, and B. Vucetic, "Joint beamforming and user association scheme for full-dimension massive MIMO networks," *IEEE Transactions on Vehicular Technology*, vol. 68, no. 8, pp. 7733–7746, Aug. 2019, doi: 10.1109/TVT.2019.2923415.
- [4] E. Björnson, L. Sanguinetti, H. Wymeersch, J. Hoydis, and T. L. Marzetta, "Massive MIMO is a reality—what is next?," *Digital Signal Processing*, vol. 94, pp. 3–20, Nov. 2019, doi: 10.1016/j.dsp.2019.06.007.
- [5] M. H. Wali, A. K. Jassim, and H. M. Almgotir, "Design and analysis 5G mobile network model to enhancement high-density subscribers," *Bulletin of Electrical Engineering and Informatics*, vol. 10, no. 3, pp. 1464–1474, Jun. 2021, doi: 10.11591/eei.v10i3.2107.
- [6] D. K. Raheja, B. K. Kanaujia, and S. Kumar, "Compact four-port MIMO antenna on slotted-edge substrate with dual-band rejection characteristics," *International Journal of RF and Microwave Computer-Aided Engineering*, vol. 29, no. 7, pp. 1–10, Jul. 2019, doi: 10.1002/mmce.21756.
- [7] M. N. Naik and H. G. Virani, "A compact four port MIMO antenna for millimeterwave applications," *Bulletin of Electrical Engineering and Informatics*, vol. 11, no. 2, pp. 878–885, Apr. 2022, doi: 10.11591/eei.v11i2.3689.
- [8] S. A. Busari, K. M. S. Huq, S. Mumtaz, L. Dai, and J. Rodriguez, "Millimeter-wave massive MIMO communication for future wireless systems: a survey," *IEEE Communications Surveys & Tutorials*, vol. 20, no. 2, pp. 836–869, 2018, doi: 10.1109/COMST.2017.2787460.
- [9] S. Kutty and D. Sen, "Beamforming for millimeter wave communications: an inclusive survey," *IEEE Communications Surveys & Tutorials*, vol. 18, no. 2, pp. 949–973, 2016, doi: 10.1109/COMST.2015.2504600.
- [10] S. S. Ioushua and Y. C. Eldar, "A family of hybrid analog–digital beamforming methods for massive MIMO systems," *IEEE Transactions on Signal Processing*, vol. 67, no. 12, pp. 3243–3257, Jun. 2019, doi: 10.1109/TSP.2019.2911255.
- [11] I. Ahmed *et al.*, "A survey on hybrid beamforming techniques in 5G: architecture and system model perspectives," *IEEE Communications Surveys & Tutorials*, vol. 20, no. 4, pp. 3060–3097, 2018, doi: 10.1109/COMST.2018.2843719.
- [12] F. F. Shareef and M. J. A. -Kindi, "Wideband hybrid precoder for mmWave multiuser MIMO OFDM communications," *Bulletin of Electrical Engineering and Informatics*, vol. 11, no. 3, pp. 1409–1417, Jun. 2022, doi: 10.11591/eei.v11i3.3551.
- [13] F. Khalid, "Hybrid beamforming for millimeter wave massive multiuser MIMO systems using regularized channel






- diagonalization," *IEEE Wireless Communications Letters*, vol. 8, no. 3, pp. 705–708, Jun. 2019, doi: 10.1109/LWC.2018.2886882.
- [14] E. Ali, M. Ismail, R. Nordin, and N. F. Abdulah, "Beamforming techniques for massive MIMO systems in 5G: overview, classification, and trends for future research," *Frontiers of Information Technology & Electronic Engineering*, vol. 18, no. 6, pp. 753–772, Jun. 2017, doi: 10.1631/FITEE.1601817.
- [15] V. V. Ratnam and A. F. Molisch, "Periodic analog channel estimation aided beamforming for massive MIMO systems," *IEEE Transactions on Wireless Communications*, vol. 18, no. 3, pp. 1581–1594, Mar. 2019, doi: 10.1109/TWC.2019.2893670.
- [16] Y. Niu, Y. Li, D. Jin, L. Su, and A. V. Vasilakos, "A survey of millimeter wave communications (mmWave) for 5G: opportunities and challenges," *Wireless Networks*, vol. 21, no. 8, pp. 2657–2676, Nov. 2015, doi: 10.1007/s11276-015-0942-z.
- [17] X. Zhang, A. F. Molisch, and S. -Y. Kung, "Variable-phase-shift-based RF-baseband codesign for MIMO antenna selection," *IEEE Transactions on Signal Processing*, vol. 53, no. 11, pp. 4091–4103, Nov. 2005, doi: 10.1109/TSP.2005.857024.
- [18] C. Hu, Y. Liu, L. Liao, and R. Zhang, "Hybrid beamforming for multi-user MIMO with partially-connected RF architecture," *IET Communications*, vol. 13, no. 10, pp. 1356–1363, Jun. 2019, doi: 10.1049/iet-com.2018.5830.
- [19] M. Li, Z. Wang, H. Li, Q. Liu, and L. Zhou, "A hardware-efficient hybrid beamforming solution for mmWave MIMO systems," *IEEE Wireless Communications*, vol. 26, no. 1, pp. 137–143, Feb. 2019, doi: 10.1109/MWC.2018.1700391.
- [20] R. W. Heath, N. G. -Prelcic, S. Rangan, W. Roh, and A. M. Sayeed, "An overview of signal processing techniques for millimeter wave MIMO systems," *IEEE Journal of Selected Topics in Signal Processing*, vol. 10, no. 3, pp. 436–453, Apr. 2016, doi: 10.1109/JSTSP.2016.2523924.
- [21] O. E. Ayach, S. Rajagopal, S. A. -Surra, Z. Pi, and R. W. Heath, "Spatially sparse precoding in millimeter wave MIMO systems," *IEEE Transactions on Wireless Communications*, vol. 13, no. 3, pp. 1499–1513, Mar. 2014, doi: 10.1109/TWC.2014.011714.130846.
- [22] P. Almers *et al.*, "Survey of channel and radio propagation models for wireless MIMO systems," *EURASIP Journal on Wireless Communications and Networking*, vol. 2007, no. 1, pp. 1–19, Dec. 2007, doi: 10.1155/2007/19070.
- [23] E. Vlachos, G. C. Alexandropoulos, and J. Thompson, "Wideband MIMO channel estimation for hybrid beamforming millimeter wave systems via random spatial sampling," *IEEE Journal of Selected Topics in Signal Processing*, vol. 13, no. 5, pp. 1136–1150, Sep. 2019, doi: 10.1109/JSTSP.2019.2937633.
- [24] Y. -P. Lin, "Hybrid MIMO-OFDM beamforming for wideband mmWave channels without instantaneous feedback," *IEEE Transactions on Signal Processing*, vol. 66, no. 19, pp. 5142–5151, Oct. 2018, doi: 10.1109/TSP.2018.2864610.
- [25] M. Alouzi and F. Chan, "Millimeter wave massive MIMO with Alamouti code and imperfect channel state information," in *2018 IEEE 5G World Forum (5GWF)*, Jul. 2018, pp. 507–511, doi: 10.1109/5GWF.2018.8516942.
- [26] A. A. M. Saleh and R. Valenzuela, "A statistical model for indoor multipath propagation," *IEEE Journal on Selected Areas in Communications*, vol. 5, no. 2, pp. 128–137, Feb. 1987, doi: 10.1109/JSAC.1987.1146527.
- [27] T. Choudhary, A. Kumar, and P. K. Raghuvanshi, "Implementation of orthogonal frequency division multiplexing for frequency selective fading channels," in *2014 International Conference on Electronics and Communication Systems (ICECS)*, Feb. 2014, pp. 1–4, doi: 10.1109/ECS.2014.6892775.
- [28] Z. Li, S. Han, and A. F. Molisch, "Hybrid beamforming design for millimeter-wave multi-user massive MIMO downlink," in *2016 IEEE International Conference on Communications (ICC)*, May 2016, pp. 1–6, doi: 10.1109/ICC.2016.7510845.
- [29] A. Adhikary, J. Nam, J. -Y. Ahn, and G. Caire, "Joint spatial division and multiplexing—the large-scale array regime," *IEEE Transactions on Information Theory*, vol. 59, no. 10, pp. 6441–6463, Oct. 2013, doi: 10.1109/TIT.2013.2269476.
- [30] T. A. Nugraha, I. Surahmat, and F. Firdaus, "Block diagonalization precoding and power allocation for clustering small-cell networks," *Bulletin of Electrical Engineering and Informatics*, vol. 9, no. 6, pp. 2364–2370, Dec. 2020, doi: 10.11591/eei.v9i6.2580.
- [31] T. Kailath, A. H. Sayed, and B. Hassibi, *Linear estimation*. New Jersey, USA: Prentice Hall, 2000.

## BIOGRAPHIES OF AUTHORS



**Faez Fawwaz Shareef**    is received the bachelor's degree in Communication Engineering from University of Technology, Iraq in 2002 and the master degree in Communication Engineering from University of Technology, Iraq in 2004. He is an Assistant Lecturer at the Department of Communication Engineering, University of Technology, Iraq since 2005. He is a Ph.D. student at the Department of Electronic and Communication Engineering, Al-Nahrain University. His research interests include cognitive radio, 5G systems, massive MIMO, beamforming, and digital signal processing. He can be contacted at email: faez.f.shareef@uotechnology.edu.iq.



**Manal Jamil Al-Kindi**    is Assistant Professor at the Department of Electronic and Communication Engineering, Al-Nahrain University, Iraq, where he has been a faculty member since 1998. He was also Head of the Department Electronic and Communications Engineering, College of Engineering, Al-Nahrain University. He graduated B.Sc. degree from Department Electrical and Electronic Engineering, University of Technology, Iraq in 1978, and completed his Ph.D. from Department of Electronic and Electrical Engineering/Communications group, University of Strathclyde/Glasgow, U.K in 1988. His research interests are primarily in the area of digital signal processing, adaptive communication system, channel estimation, and noise cancelation. He can be contacted at email: manal.jamil.1@nahrainuniv.edu.iq.